Supporting Information

Dual-Emission Fluorescence Coordination Polymer for Simultaneous Quantification of Al^{3+} and Pb^{2+} in Their Mixtures

Xiaomei Wang, Yufen Li, Lanqing Liu, Zhenqi Tan, Xinhui Zhou, Yujian You, Shi Wang*

State Key Laboratory of Organic Electronics and Information Displays & Institute of Advanced Materials (IAM), Nanjing University of Posts & Telecommunications, Nanjing 210023, China

E-mail addresses: *iamxhzhou@njupt.edu.cn (X. Zhou)

Instrumentation

A Bruker D8-advance X-ray diffractometer equipped with Cu-Kα (λ = 1.5418 Å) radiation was used to obtain PXRD data collected in the 5–50° range of 2θ with a scan step width of 0.02°. Photoluminescence spectra were obtained using an RF-6000 Plus fluorescence spectrophotometer. The UV–Vis absorption spectra of the samples were collected using a PerkinElmer Lambda 35. The fluorescence lifetime curves were obtained using an Edinburgh FLS920 spectrophotometer. X‑ray photoelectron spectroscopy (XPS) was acquired by X-ray photoelectron spectroscopy (Axis Supra) with Al Kα radiation. An inductively coupled plasma mass spectrometer (ICP-MS) (NEXION 2000, PerkinElmer) was used for obtaining the concentrations of Al^{3+} and Pb^{2+}.

Table S1. Sensing performance of different materials toward Al^{3+} ions

Al^{3+} sensors	LOD	Reference
1	**33.8 nM**	**This study**
$\{[InZn_2(cbda)_2(H_2O)_2](NMF)_3\}_n$	0.56 μM	Ref[1]
$[Eu(atpt)_{1.5}(phen)(H_2O)]_n$	10 μM	Ref[2]
$\{[Tb(Cmdcp)(H_2O)_3]_2(NO_3)_2\cdot 5H_2O\}_n$	6.6 μM	Ref[3]
$[Zn(NH_2\text{-bdc})(4,4'\text{-bpy})]$	30 nM	Ref[4]
UiO-$(OH)_2$@RhB	10 nM	Ref[5]
$\{Zn(Dpada)(Imdba)\cdot H_2O\}_n$	0.69 μM	Ref[6]
Eu-BDC-NH_2/TDA	0.14 μM	Ref[7]
$[Zn(H_2dhbdc)(Cz\text{-}3,6\text{-bpy})]_n$	0.62 μM	Ref[8]

LOD: limit of detection; H_4cbab: 5,5′-(carbonylbis(azanediyl))-diisophthalic acid;

NMF: *N*-methylformamide; H_2atpt: 2-aminoterephthalic acid;

phen: 1,10-phenanthroline; H_3CmdcpBr: *N*-carboxymethyl-(3,5-dicarboxyl)pyridinium bromide

NH_2-H_2bdc: 2-amino-1,4-benzenedicarboxylic acid; 4,4′-bpy: 4,4′-bipyridine

RhB: rhodamine B; Dpada: 3, 6-di(1*H*-imidazol-1-yl) pyridazine

Imdba: 2, 2′-iminodibenzoic acid; BDC-NH_2: 2-aminoterephthalic acid;

TDA: 2,5-thiophenedicarboxylic acid; H_4dhbdc: 2,5-dihydroxyterephthalic acid;

Cz-3,6-bpy: 3,6-bis(pyridin-4-yl)-9*H*-carbazole

Table S2. Sensing the performance of different materials toward Pb^{2+} ions

Pb^{2+} sensors	LOD	Reference
1	**30.0 nM**	**This study**
NH_2-Ni-MOF	0.2 nM	Ref[9]
MOF-5-NH_2	0.25 μM	Ref[10]
$Zn_4O(TPA)_3$	2 nM	Ref[11]
$[Tb(L)(H_2O)_5]_n$	0.1 μM	Ref[12]
Co-TMC4R- BDC	11 nM	Ref[13]

MOF: Metal Organic Framework; TPA: terephthalic acid;

H_2L^-: 3, 5-dicarboxy-phenol anion ligand;

TMC4R: tetra(4-mercaptopyridine)calix[4]resorcinarene; 1,4-BDC: 1,4-benzenedicarboxylic acid

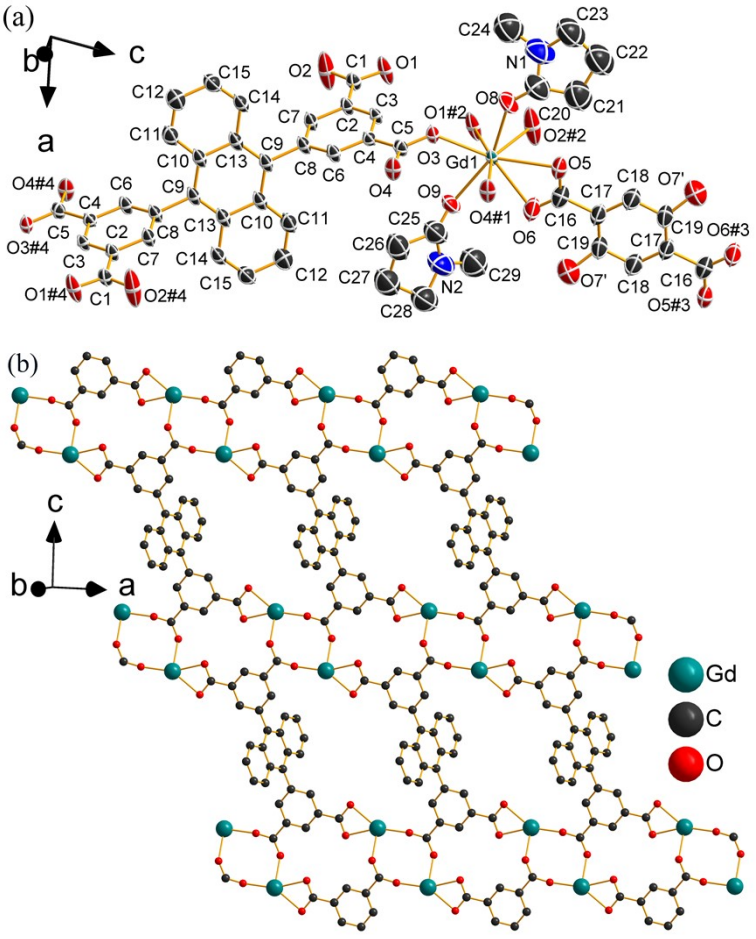

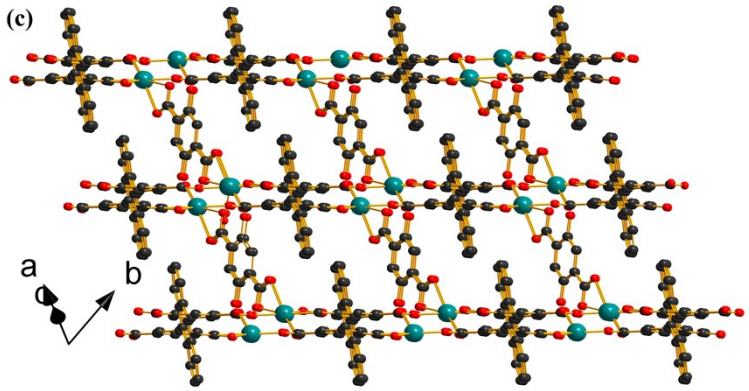

Fig. S1 (a) Under the thermal ellipsoids drawn at the 50% probability level, the asymmetric unit of **1**. (b) The 2D coordination network is located on (111) crystal plane. (c) The 3D framework of **1**. For clarity, all hydrogen atoms in (a), (b), (c), and NMP molecules in (b), (c) are omitted. Symmetry codes: $^{\#1}$-x+2, -y, -z+1; $^{\#2}$-x+1, -y+1, -z+1; $^{\#3}$-x+2, -y, -z+2; $^{\#4}$-x+2, -y+1, -z.

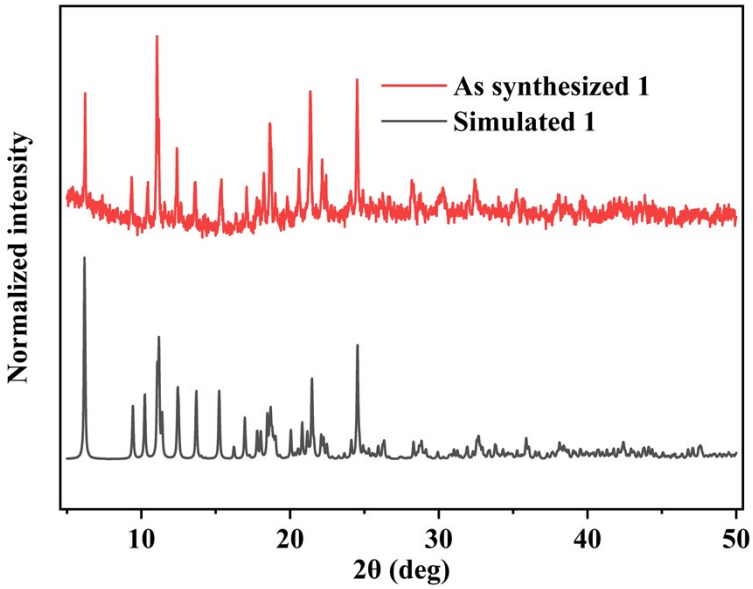

Fig. S2 The PXRD patterns of **1**.

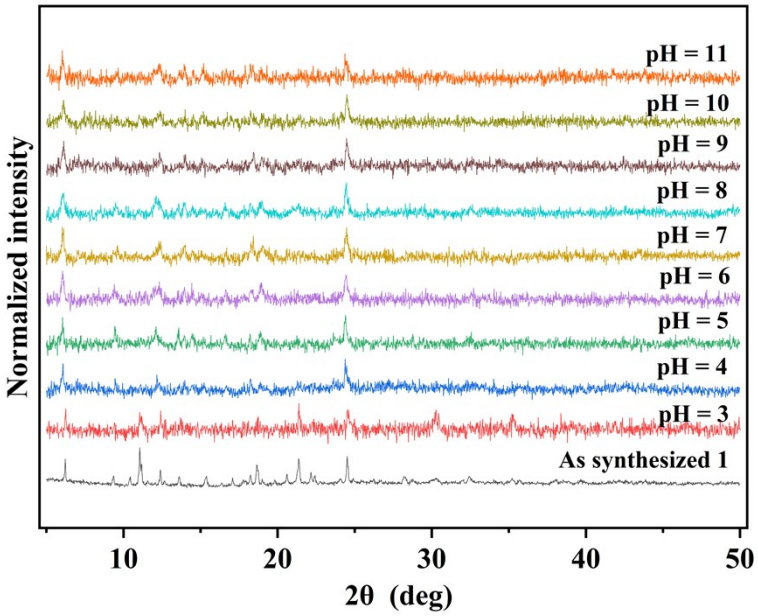

Fig. S3 PXRD diagram of **1** in different pH values.

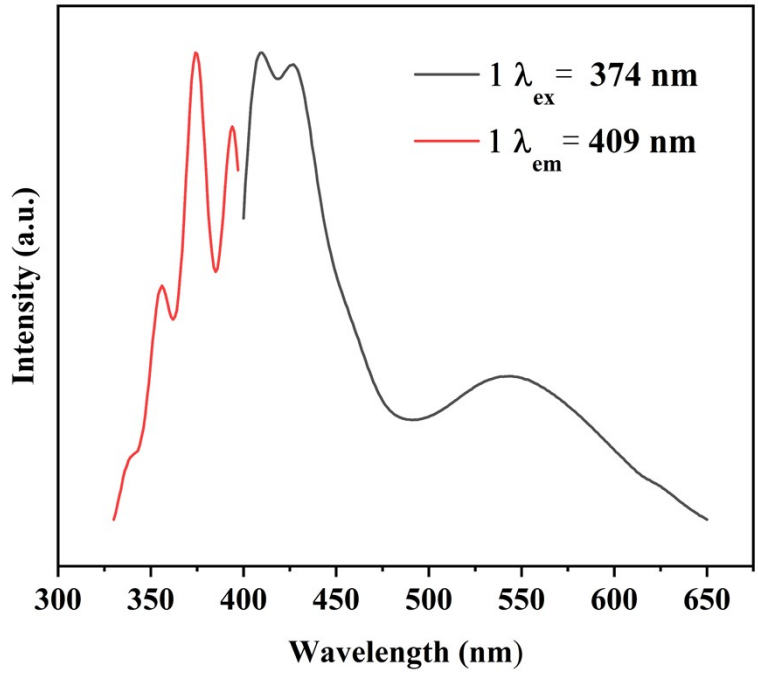

Fig. S4 Excitation and emission spectra of **1** in aqueous solution.

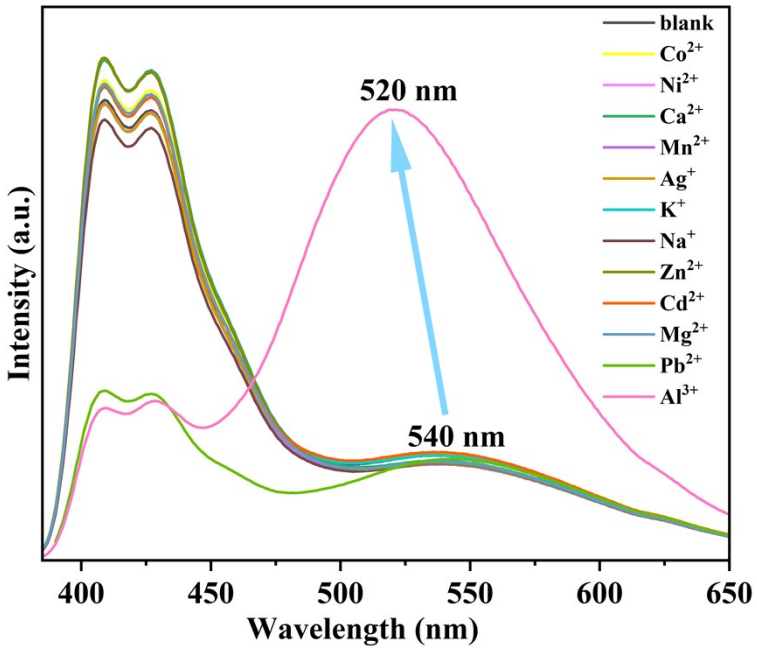

Fig. S5 Fluorescence intensity selectivity of **1**-H_2O suspension adding 9 μM different metal ions upon excitation at 374 nm

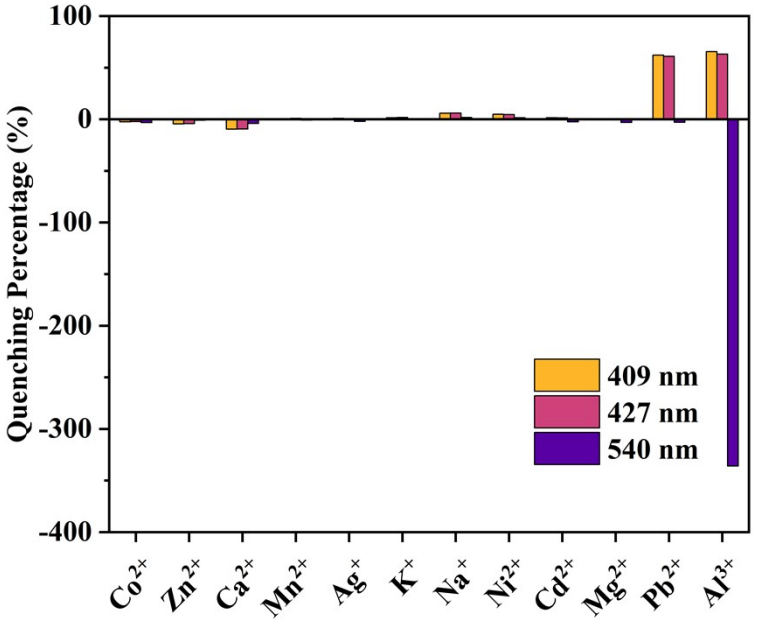

Fig. S6 Fluorescence quenching percentages of **1**-H_2O suspension for the intensities of emission peaks at 409, 427, and 540 nm after the addition of different kinds of metal ions (9 μM) upon excitation at 374 nm.

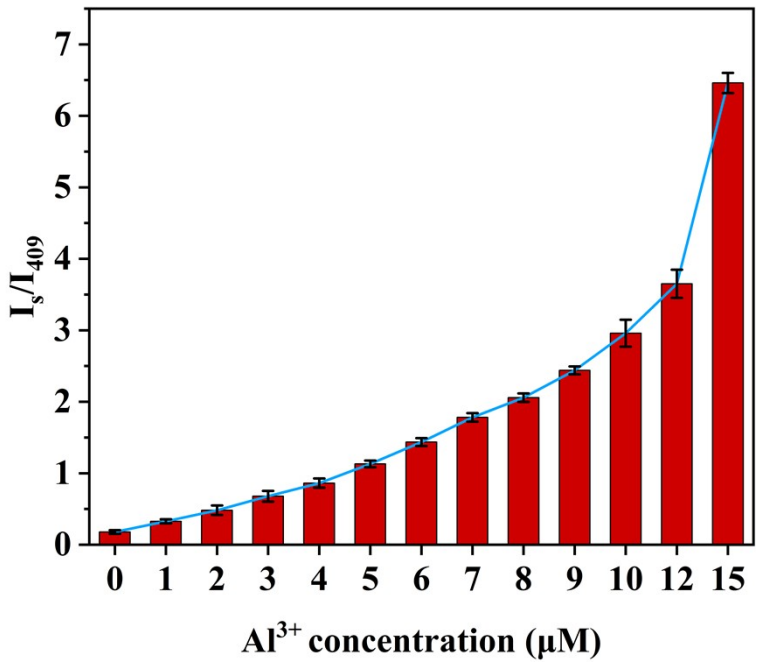

Fig. S7 Plot of I_s/I_{409} values at different concentrations of Al^{3+} ions

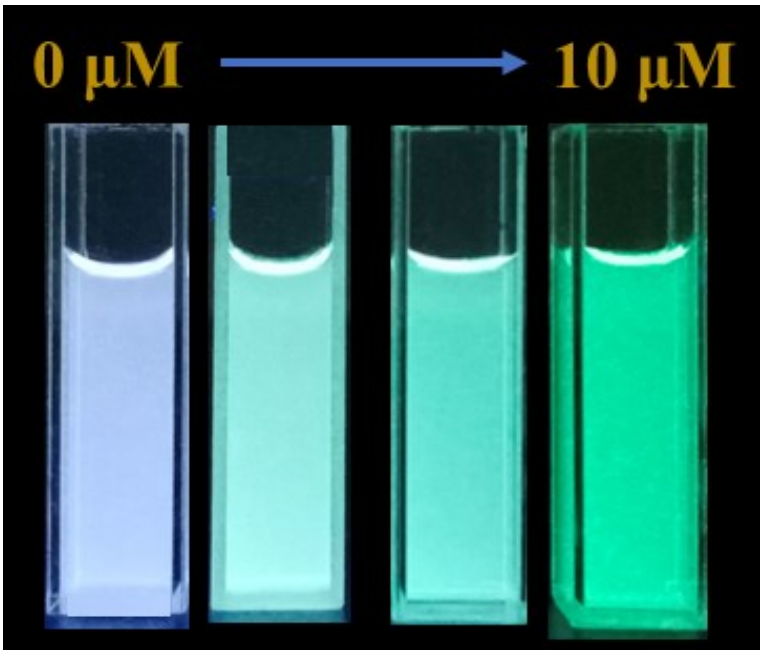

Fig. S8 Photographs of **1**-H_2O after adding different concentrations of Al^{3+} ions under UV-light irradiation at 365 nm

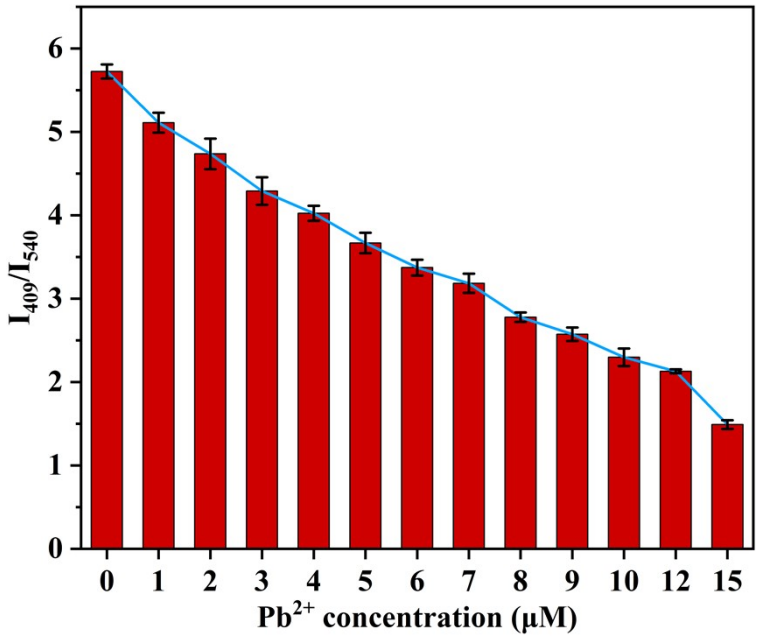

Fig. S9 Plot of I_{409}/I_{540} values at different concentrations of Pb^{2+} ions.

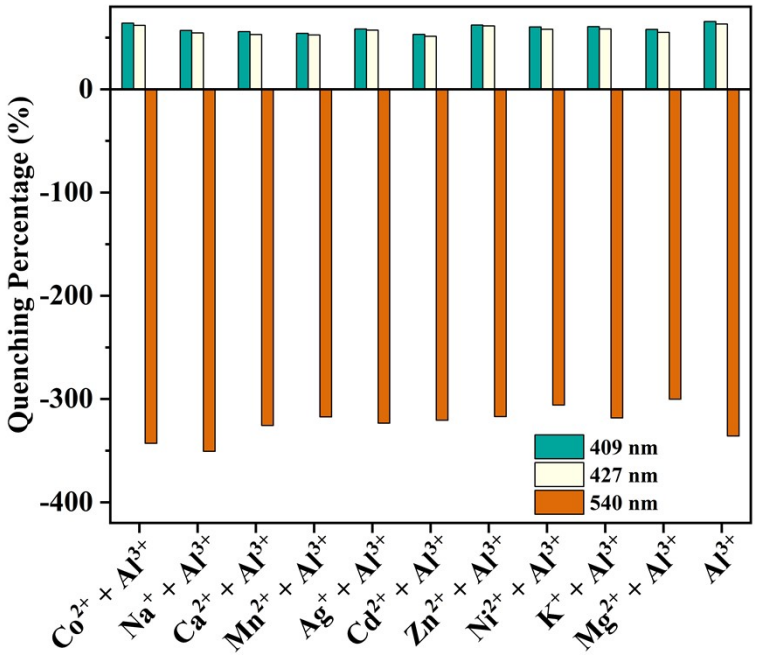

Fig. S10 Quenching percentage when **1**-H_2O suspension is treated with Al^{3+} (9 μM) and other interfering ions (90 μM)

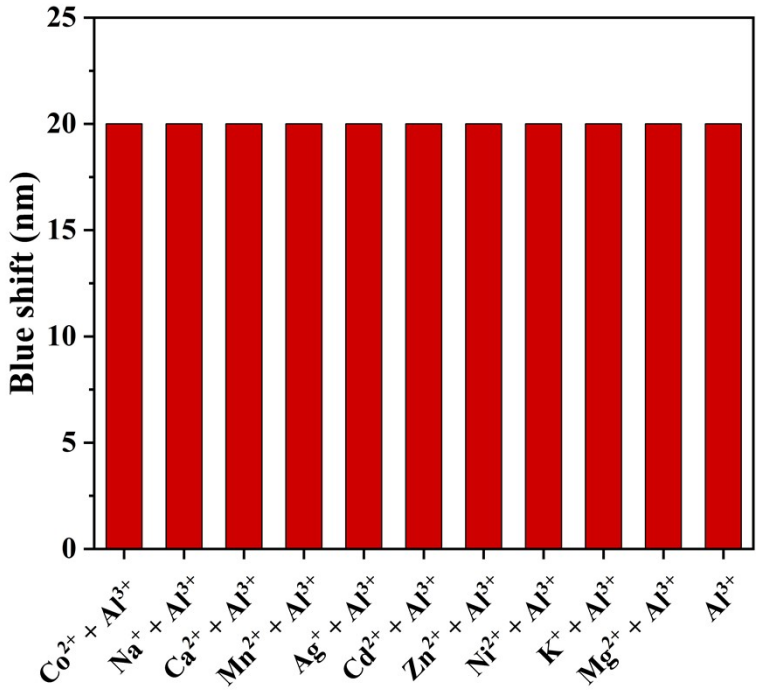

Fig. S11 Blue shift of **1**-H_2O suspension treated with Al^{3+} (9 μM) and other interfering ions (90 μM) upon excitation at 374 nm

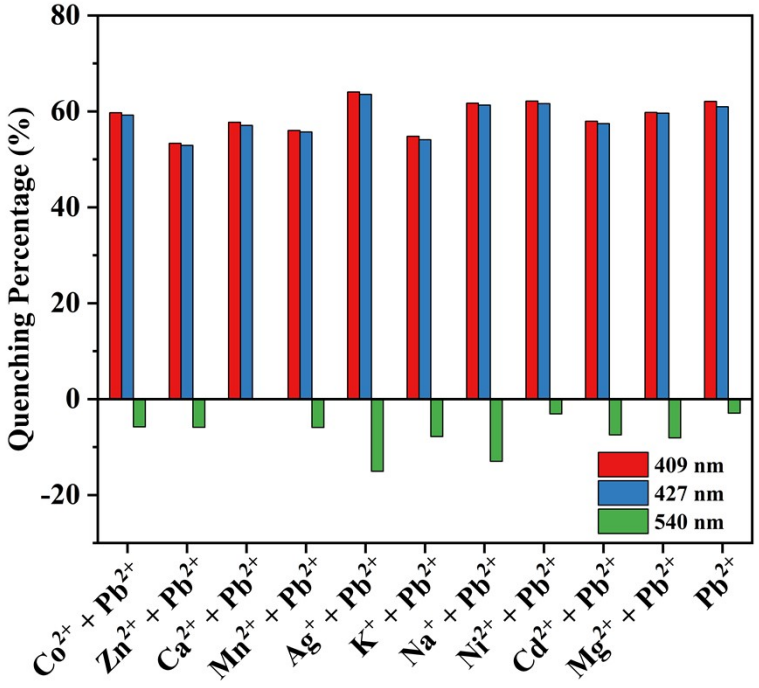

Fig. S12 Quenching percentage of **1**-H_2O suspension treated with Pb^{2+} (9 μM) and other interfering ions (90 μM)

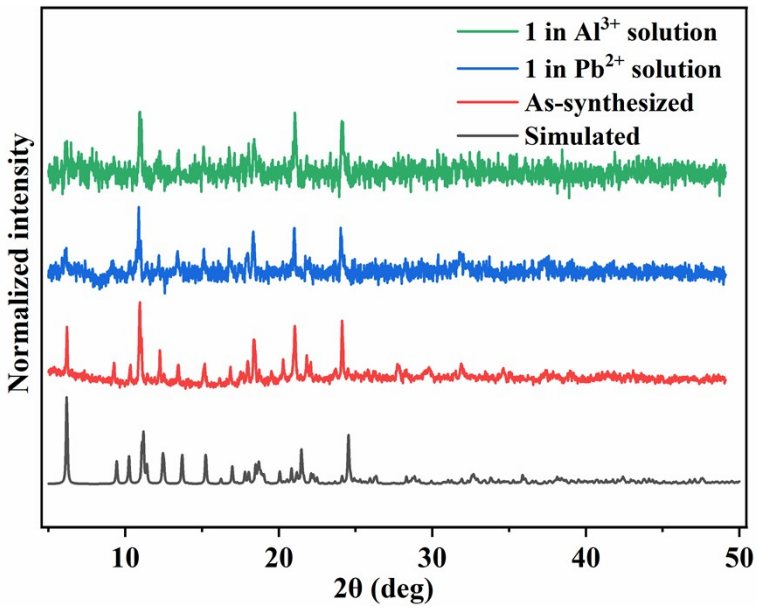

Fig. S13 Powder X-ray diffraction (PXRD) patterns of **1** in solutions containing Al^{3+} and Pb^{2+} ions

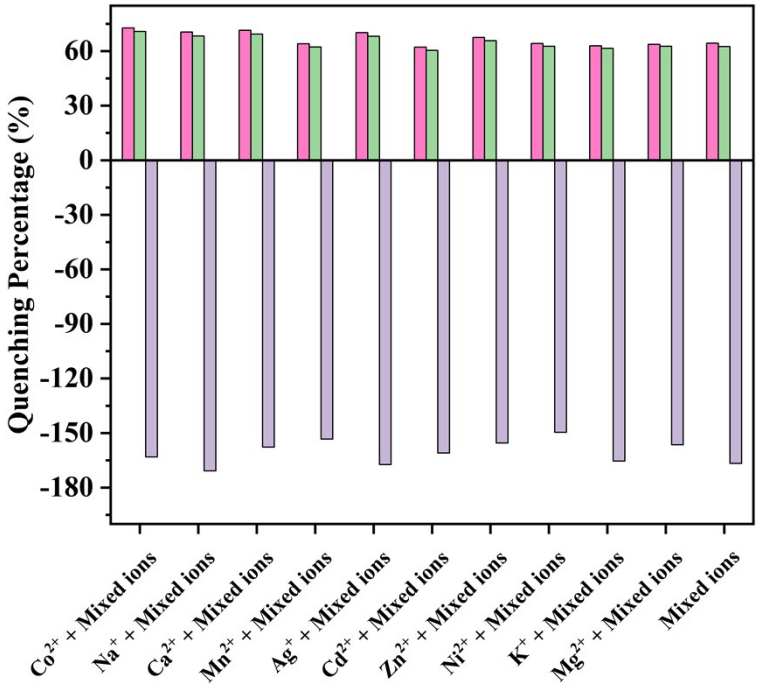

Fig. S14 Fluorescence quenching percentages of **1**-H_2O suspension treated with mixed ions (9 μM) and other interfering ions (90 μM)

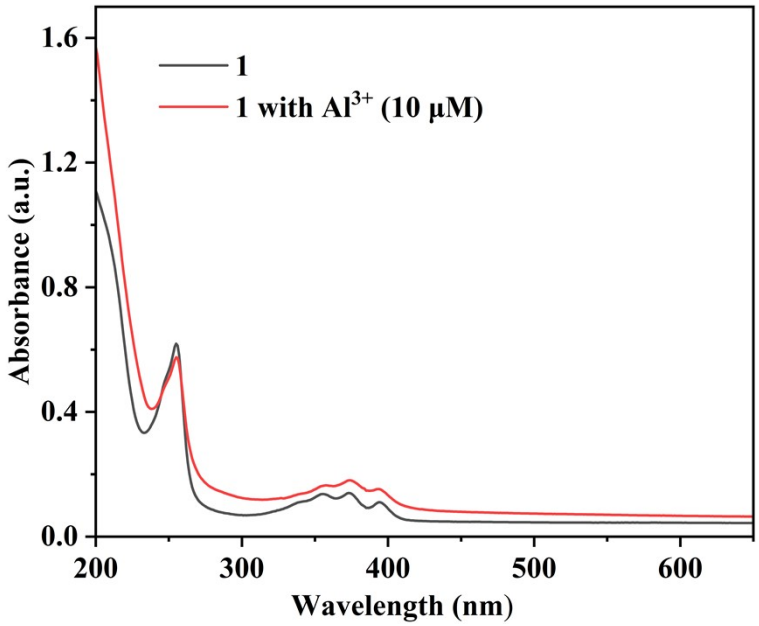

Fig. S15 UV absorption intensity of **1**-H_2O suspension after adding Al^{3+} ions

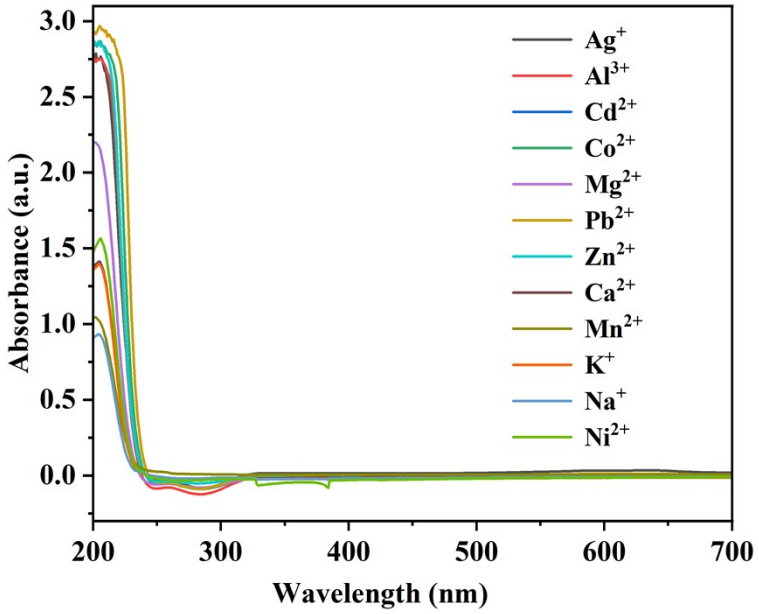

Fig. S16 UV absorption intensity of **1**-H_2O suspension after adding different metal ions

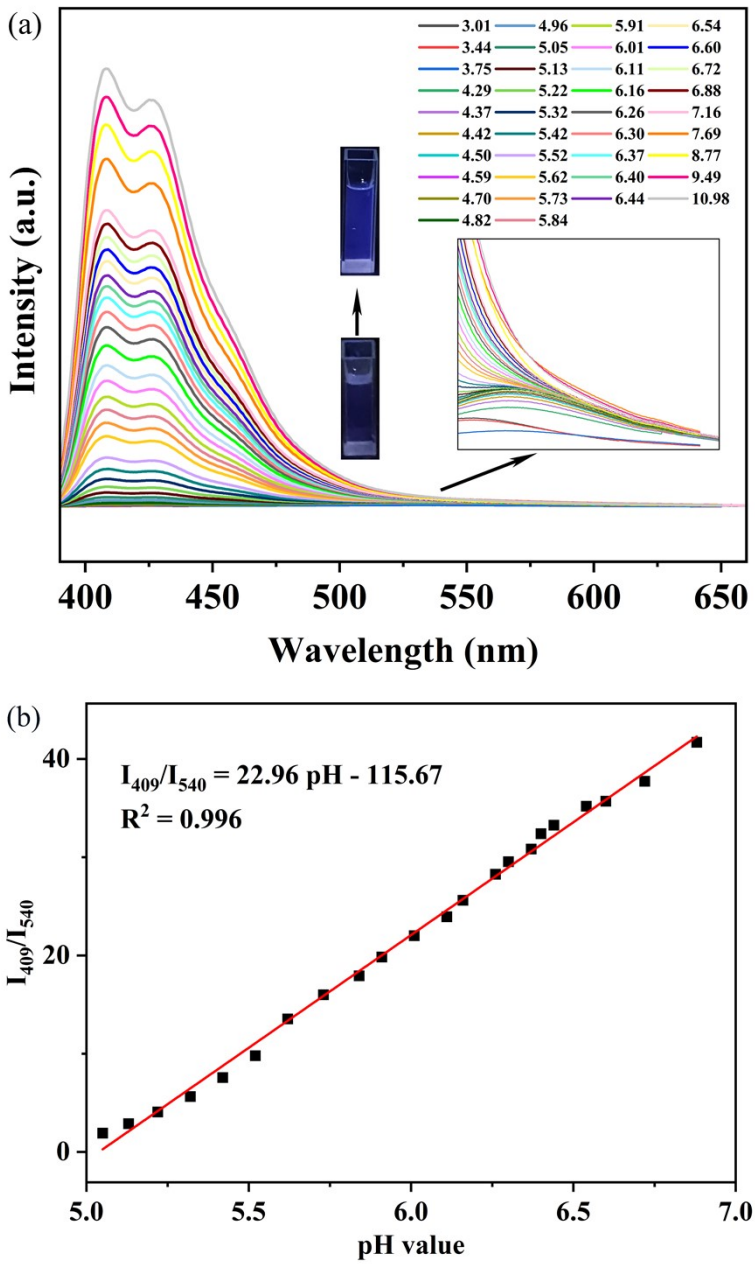

Fig. S17 (a) Emission spectra of **1**-H_2O suspension in the pH range of 3.01-10.98; inset: changes in luminescence intensity visible to the naked eye at pH 5.05-6.88 under 365 nm UV light. (b) The linear relationship between pH value and I_{409}/I_{540} (excited at 374 nm).

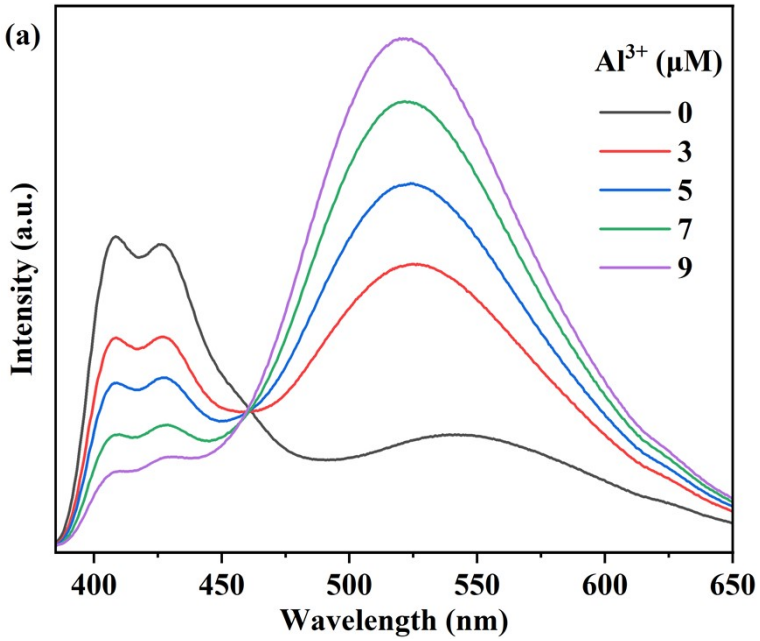
(a)
Al3+ (μM)
0
3
5
7
9
Intensity (a.u.)
400
450
500
550
600
650
Wavelength (nm)

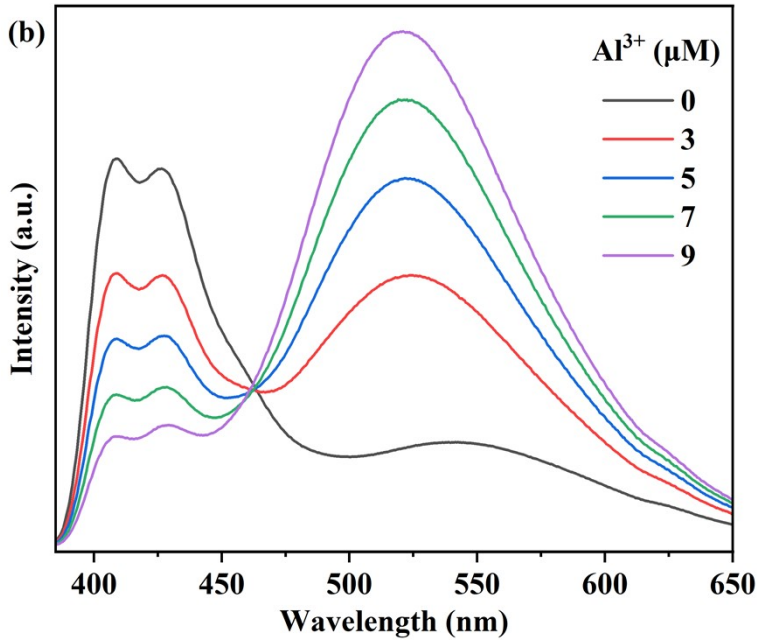
(b)
Al3+ (μM)
0
3
5
7
9
Intensity (a.u.)
400
450
500
550
600
650
Wavelength (nm)

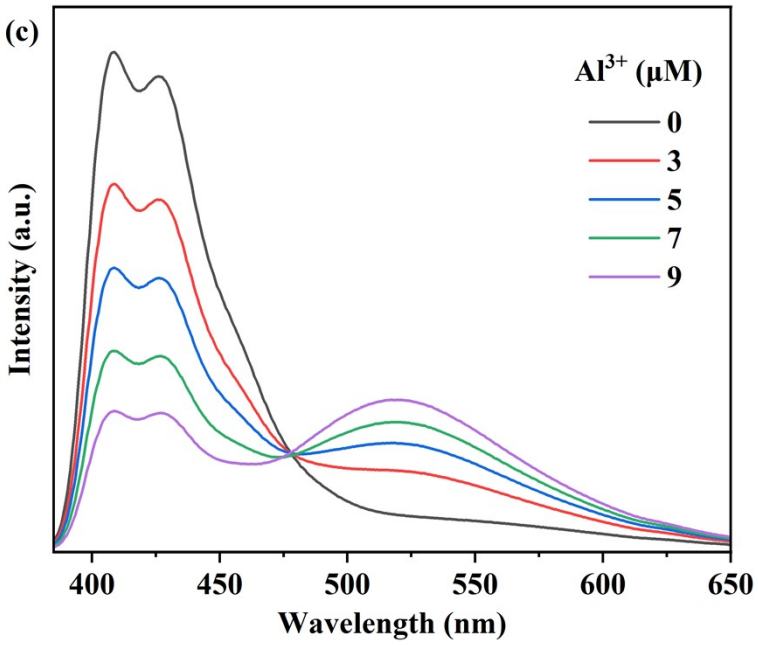

Fig. S18 Emission spectra of **1**-H_2O suspension with different concentrations of Al^{3+} ions at (a) pH = 5.23, (b) pH = 5.31, (c) pH = 5.60

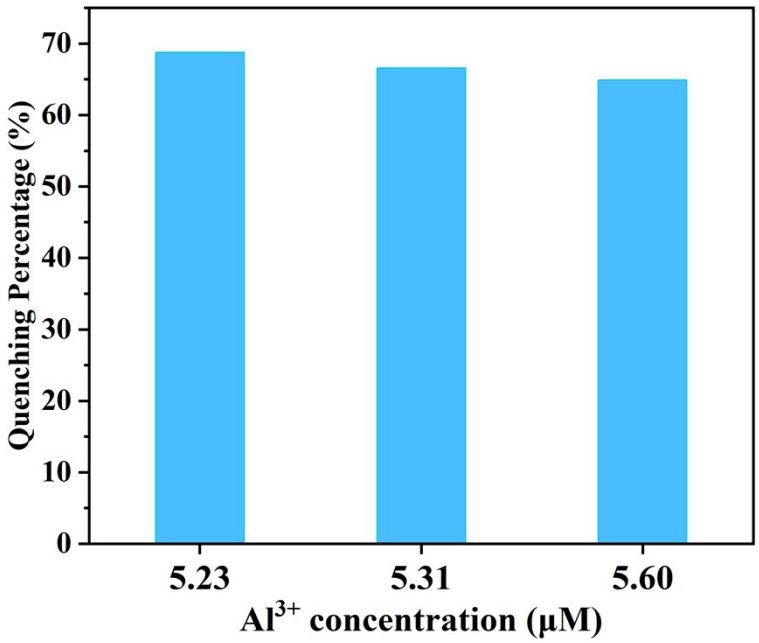

Fig. S19 Fluorescence quenching percentages of **1**-H_2O suspension for the intensities of emission peaks at 409 nm after the addition of different concentrations of Al^{3+} ions at different pH values upon excitation at 374 nm

.

References

[1] Y.-Y. Hou, L.-B. Zhou, C.-F. Meng, J. Guan, G.-L. Zhang, Y.-Z. Hou, *J. Clust. Sci*., 2020, **31**, 1285-1293.

[2] Y. Kang, X.-J. Zheng, L.-P. Jin, *J. Colloid Interface Sci.*, 2016, **471**, 1-6.

[3] M. Chen, K.-Y. Wu, W.-L. Pan, N.-H. Huang, R.-T. Li, J.-X. Chen, *Spectrochim. Acta. A Mol. Biomol. Spectrosc.*, 2021, **247**, 119084.

[4] T. Wiwasuku, J. Othong, J. Boonmak, V. Ervithayasuporn, S. Youngme, *Dalton Trans.*, 2020, **49**, 10240-10249.

[5] X. Zheng, Y. Zhao, P. Jia, Q. Wang, Y. Liu, T. Bu, M. Zhang, F. Bai, L. Wang, *Inorg. Chem.*, 2020, **59**, 18205-18213.

[6] Q. Li, S. Xu, L. He, K. Huang, X. Zhang, D. Qin, *Spectrochim. Acta. A Mol. Biomol. Spectrosc.*, 2022, **279**, 121461.

[7] R. Wang, H. Zhang, Si. Wang, F. Meng, J. Sun, D. Lou, Z. Su, *Inorg. Chem. Front.*, 2023, **10**, 1534-1542.

[8] W.-T. Chen, M.-J. Tsai, J.-Y. Wu, *Cryst. Growth Des.*, 2022, **22**, 228-236.

[9] J. Wan, Y. Shen, L. Xu, R. Xu, J. Zhang, H. Sun, C. Zhang, C. Yin, X. Wang, *J. Electroanal. Chem.*, 2021, **895**, 115374.

[10] X. An, Q. Tan, S. Pan, H. Liu, X. Hu, *Spectrochim. Acta. A Mol. Biomol. Spectrosc.*, 2021, **247**, 119073.

[11] S. Xu, L. Zhan, C. Hong, X. Chen, X. Chen, M. Oyama, *Sens. Actuators B Chem.*, 2020, **308**, 127733.

[12] G. Ji, J. Liu, X. Gao, W. Sun, J. Wang, S. Zhao, Z. Liu, *J. Mater. Chem. A*, 2017, **5**, 10200-10205.

[13] F.-F. Wang, C. Liu, J. Yang, H.-L. Xu, W.-Y. Pei, J.-F. Ma, *Chem. Eng. J.*, 2022, **438**, 135639.